

Article

Preliminary Investigation of Geopolymer Foams as Coating Materials

Krzysztof Kaczmarek, Kinga Pławecka *, Barbara Kozub , Patrycja Bazan  and Michał Łach *

Department of Materials Engineering, Faculty of Materials Engineering and Physics, Tadeusz Kosciuszko, Cracow University of Technology, Jana Pawła II 37, 31-864 Cracow, Poland

* Correspondence: kinga.plawecka@pk.edu.pl (K.P.); mlach@pk.edu.pl (M.Ł.)

Abstract: Various types of coatings are applied to the surface of an object or substrate to improve surface properties or extend service life, which in turn is associated with cost reductions. The main objective of this study was to develop a technique for the additive application of foamed geopolymers to existing structures and vertical surfaces. The base material was a fly ash-based geopolymer modified with sand. Hydrogen peroxide and aluminum powder were used as foaming agents. In this study, the feasibility of using an air gun with variable nozzles to apply the layers of foamed geopolymers was assessed, and the effects of nozzle diameter and the spray gun's operating pressure were analyzed. The next stage of the study was a visual assessment of the layering of the foamed material. The foamed geopolymer layering tests verified the occurrence of the foaming process, and the applied geopolymer surface showed a reasonably good adhesive bond with the vertical wall. In addition, in this paper, we present the laser particle size results of the base materials and their oxide composition. In addition, thermal conductivity tests for the foamed geopolymer materials, compressive strength tests, and microstructure analysis via scanning electron microscopy were carried out.

Keywords: additive technologies; geopolymer foam; geopolymer insulation; fly ash; foaming agents



Citation: Kaczmarek, K.; Pławecka, K.; Kozub, B.; Bazan, P.; Łach, M. Preliminary Investigation of Geopolymer Foams as Coating Materials. *Appl. Sci.* **2022**, *12*, 11205. <https://doi.org/10.3390/app122111205>

Academic Editors: Tomislav Ivankovic, Vanja Jurišić and Agnese Magnani

Received: 9 August 2022

Accepted: 3 November 2022

Published: 4 November 2022

Publisher's Note: MDPI stays neutral with regard to jurisdictional claims in published maps and institutional affiliations.



Copyright: © 2022 by the authors. Licensee MDPI, Basel, Switzerland. This article is an open access article distributed under the terms and conditions of the Creative Commons Attribution (CC BY) license (<https://creativecommons.org/licenses/by/4.0/>).

1. Introduction

Geopolymers are defined as inorganic materials formed due to the alkaline activation of aluminosilicates [1–3]. Naturally occurring materials, such as kaolin, metakaolin, rice husk ash, volcanic rock powders, and high calcium wood ash, are used as precursors for the production of geopolymer materials [4–7]. However, geopolymer materials are increasingly produced using post-processing waste such as fly ash or blast furnace slag [8–11]. Therefore, much research has been devoted to geopolymer materials by focusing on selecting an appropriate precursor, geopolymerization methods, process optimization, and modification of strength properties [12–21]. Geopolymer and geopolymer concrete materials are used in construction as an alternative to conventional concrete, showing high strength, increased durability, better workability, reduced permeability, and reduced shrinkage, thus limiting cracking [22].

A fundamental property of geopolymers is their significantly higher thermal resistance compared with conventional concrete. A comparison of the results of fire resistance tests showed that samples made of conventional concrete were characterized by intense cracking after exceeding 800 °C, whereas geopolymeric materials showed only slight and few cracks under the same conditions. As shown by studies at very high temperatures, no spattering was observed in the case of geopolymers. Fire resistance tests justified the use of geopolymeric materials where fire resistance and structural properties are of crucial importance, e.g., in buildings that require fireproof and protective coatings for various surfaces [23–25].

Coatings are applied to the surface of an object or substrate to improve its surface properties such as appearance, roughness, adhesion, wettability, corrosion resistance, abrasion resistance, scratch resistance, and thermal and thermomechanical resistance while maintaining or improving their mechanical and physical properties. Coatings also allow

for an increase in the service life of the structure/substrate, which in turn is associated with ease of maintenance and a reduction in refurbishment costs [26,27].

It is essential that the coating forms an integral whole with the substrate. The processes accompanying the application of alkaline-activated coatings to the substrate include water evaporation, geopolymerization, and the formation of a bond between the coating and the substrate. Maintaining the balance between these processes allows for a defect-free, integral coating characterized by strong adhesion with the substrate [27,28].

There are various methods of applying geopolymer coatings, the most common of which are dipping, spraying, blading, brushing, and extruding [29].

Applying alkaline-activated coating through the dip method is convenient and simple. However, a significant disadvantage of this method is the inability to accurately control the thickness of the applied layer. Temuujin et al. used a simple dipping method to study metakaolin-based geopolymer coatings. Geopolymer paste was applied to stainless and soft steel substrates. The steel surfaces were previously prepared by cleaning with sandpaper, washing with a detergent, and degreasing with acetone. The geopolymer was applied to metal substrates by dipping the steel into a geopolymer mix. In this method, the viscosity of the geopolymer paste is an important factor. It must flow freely, and its properties depend on the water content. The coating thickness obtained through this method was approximately 0.3–0.8 mm. After applying the geopolymer pastes to the metal surface, the samples were cured at 70 °C for 24 h. The study of the coating properties showed that the adhesive properties of the metakaolin-based geopolymer to the steel of the substrate depended on their chemical composition. The adhesion strength was determined at the level of >3.5 MPa. This research showed the significance of Si:Al and Na:Al ratios. The best results were obtained with the ratios of Si:Al = 2.5 and Na:Al = 1 [29].

Geopolymer coatings applied through the dipping or brushing method make the obtained coatings relatively thick, which may limit their use in the case of applications in which layers of small thickness are required to minimize, for example, the possibility of mismatched properties between the coating and the substrate [30].

The spray method is much more precise. The use of this dosing method ensures the precise and reproducible atomization of low-flow, high-viscosity media. The geopolymer is fed to the screw from a dispenser with an air supply pressure of about 1 bar. This ensures a flow of the material into the screw cavity regardless of the orientation of the atomizer. This process consists of making quick sweeping movements and applying a few dozen thin layers of the coating material. It is then carried out, cured for 28 days at room temperature, and immersed in a water tank. This method allows for more accurate coverage of the substrate and enables small holes in the concrete surface to be filled with material. The main advantages of the spray method include low cost, efficiency, the ability to control the thickness of the applied layer, and the ability to regulate the pressure of the airbrush. The resulting coatings are uniform and have good stability and strong adhesion to the substrate. However, in the spraying method, it is necessary to ensure that the coating suspension is flowable enough [31,32].

In their research, Zhang et al. showed that using alkaline-activated materials as inorganic coatings can be successfully used to protect sea concrete. The geopolymer mortar used in this previous study was based on metakaolin and slag with the addition of MgO and polypropylene fibers, while a sodium-based solution was used as an activator. Using a blading method, the geopolymer coating was manually applied to the previously cleaned concrete surfaces of an acropolis located along the coast. After about 30 min, wet straw mats were applied to the geopolymer layer and removed after the layer had completely solidified. The disadvantage of using this method in atmospheric conditions is the high rate of shrinkage in geopolymer paste and the formation of microcracks on the surface. However, it was found that the main factors influencing the quality and coherence of the coating were the ambient humidity and the thickness of the applied layer; the best results were obtained for a 5 mm thick layer in the tidal area (i.e., with periodic contact with seawater) [32].

Deshmukh et al. researched geopolymeric coatings based on fly ash with various silicate-to-alkali ratios ranging from 0.5 to 2.5. The studied geopolymer layers were applied with a brush to the surfaces of cleaned mild steel plates. The conducted tests showed that the tested material had promising mechanical properties, fire resistance, and corrosion resistance [33].

Bhardwaj et al. researched geopolymer coatings based on fly ash–metakaolin–phosphate. The coating was deposited on a mild steel substrate using the spin-coating method to improve the substrate–matrix interaction. The spin-coating method produced a well-ordered thin geopolymer coating (thickness 13–20 μm), despite the use of clearly thick materials. The maximum adhesion force of the material to the substrate was 2.5 MPa. This research also showed the influence of parameters such as spin speed and time. A low spin speed limits the homogeneous spread of the geopolymer, which leads to incomplete material coverage. On the other hand, too short or too long centrifugation time adversely affects the thickness and efficiency of the coating [34].

After conducting the literature review, the authors decided to apply a geopolymer layer using the spray application method, which shows the highest application potential for foamed geopolymers. This method, as mentioned earlier, allows for a more accurate application of the layer to the substrate, compared with other methods reported in the literature. However, it should be noted that the final properties of geopolymer coatings, mortars, and concrete, in addition to the method of application, are determined by other factors, including the adhesion of the geopolymer material, which in turn strongly depends on the chemical composition of the raw materials, geopolymer composition, type of substrate, surface roughness, or water content [35].

The purpose of the present study was to test the applicability of additive technology for applying foamed geopolymers to existing structures and vertical surfaces. Most applications of foamed geopolymers are based on the installation/application of molded slabs. In this case, difficulties arise in protecting surfaces with variable geometries and curvatures. Spray application technology eliminates the problem of securing irregular geometries and contributes to the use of geopolymers as an insulation material, replacing commonly used combustible insulation materials. This work focused on investigating the feasibility of using an air gun with variable nozzles to apply layers of foamed geopolymers and assessing the adhesion of the applied material to the substrate and the degree of foaming in the applied geopolymer layers on a vertical surface.

2. Materials and Methods

2.1. Materials

Fly ash from a heat and power plant in Skawina (Poland) was used as a precursor for the production of geopolymers. Fly ash was mixed with river sand (KSM Kobylice, Poland). The alkaline activator was a solution of 10 M sodium hydroxide and R-145 (sodium) water glass with a molar modulus of 2.5 and a density of approximately 1.45 g/cm^3 . An aqueous solution of sodium hydroxide with a specified concentration was mixed with the water glass in a weight ratio of 1:2.5. The solution was prepared as follows: Flakes of technical hydroxide were dissolved in water, and then an aqueous solution of sodium silicate was added. The applied foaming agents were hydrogen peroxide (perhydrol 36%, Biomus) and aluminum powder (powder, max. particle size 52 microns, purity min. 92%, BENDA-LUTZ). Before the tests with the foamed material, the appropriate consistency of the geopolymer paste was verified. The consistency of the geopolymer paste was visually assessed, and the best option was chosen, which we felt had the best fluidity and curing time and gave the best foaming effect when applied to the surface. The proportion of geopolymer ingredients was regulated by the amount of liquid part relative to the dry portion. The amount of the alkaline solution was gradually reduced until the consistency and density of the geopolymeric mass were adequate for proper spraying. The exact composition of the mixtures and their proportions by weight (L—liquid, S—solid, F—foaming agent) are given in Table 1.

Table 1. The proportion of geopolymer mass.

Index	Description	Alkaline Activator	Foaming Agent	Mix Proportion (L/S/F)
Mix 1	Geopolymer based on fly ash and river sand (weight ratio: 1:0.1)	10 M NaOH + sodium water glass (weight ratio: 1:2.5)	H ₂ O ₂	1:2.18:0.17
Mix 2	Geopolymer based on fly ash and river sand (weight ratio: 1:0.1)	10 M NaOH + sodium water glass (weight ratio: 1:2.5)	Aluminum powder	1:1.87:0.004

After obtaining the appropriate consistency of the geopolymeric mass, we focused on selecting the nozzle diameter and spray pressure. The spraying process was carried out using an AD-80030P spray gun (ADLER, Łódź, Poland), which was compatible with an FB 150-3-S AIR FORCE piston compressor (ELEKTROMIX, Chełm, Poland). The nozzles with a diameter of 4×10^{-3} , 6×10^{-3} , and 8×10^{-3} m were selected for the tests. The injection pressure was found to range from 0.4 to 0.8 MPa.

The optimization of the spraying parameters allowed for the application of foamed geopolymer materials. Table 2 shows the parameters for the possible spray nozzle ranges.

Table 2. Technical specifications of the spray gun.

Type	Manufacturer	Tank Capacity (m ³)	Nozzle Diameter (m)	Working Pressure (MPa)	Diameter of Compressed Air Supply hose (m)
Spray gun—AD-8030P	ADLER	0.005	0.004	0.4–0.8	0.008
Spray gun—AD-8030P	ADLER	0.005	0.006	0.4–0.8	0.008
Spray gun—AD-8030P	ADLER	0.005	0.008	0.4–0.8	0.008

Table 3 shows the pressure ranges for spray nozzle operation.

Table 3. Working pressure range for spray nozzle.

Spray Gun Mode	Pressure Range (MPa)
Low pressure	0.4–0.5
Medium pressure	0.51–0.65
High pressure	0.66–0.8

The selection of the optimum pressure range of the cup gun for geopolymer spraying is described in the Section 2.2.

2.2. Method of Testing

The density distribution, cumulative distributions, and mean size of the particles of base materials were analyzed using a PSA 1190 LD Particle Size Analyzer, Anton Paar (Austria).

The oxide composition was determined using the XRF method with a PANalytical Epsilon spectrometer, following PN-EN 1744-1 + A1: 2013-05.

The heat conduction coefficient was tested on the HFM 446 plate apparatus (Witelsbacherstrasse, Germany). In a heat flow meter (HFM), the test specimen was placed between two heated plate-controlled temperatures. For the tests, panels with dimensions of approximately $200 \times 200 \times 25$ mm were made.

Compressive strength tests were performed according to EN 12390-3 (“Testing of hardened concrete. Compressive strength of specimens”) on cubic specimens ($50 \text{ mm} \times 50 \text{ mm} \times 50 \text{ mm}$) using a Matest 3000 kN testing machine (Matest, Treviolo, Italy). In the compression test, 10 specimens of geopolymer were tested. The results obtained are average values.

Microscopic observations were carried out using a JEOL JSN5510LV scanning electron microscope (JEOL Ltd., Tokyo, Japan). The samples were used for testing after mechanical property tests. Before testing, the surface of the sample was coated with a conductive gold layer on a JOEL JEE-4X vacuum evaporator (JEOL Ltd., Tokyo, Japan).

3. Results and Discussion

In the first stage, the geopolymerization process consisted of dissolving the base materials, breaking the bonds between silicon and oxygen and between aluminum and oxygen, and then starting the polycondensation process, after which a three-dimensional structure was created. The most important components of the materials susceptible to the geopolymerization process were the presence of silicon and aluminum. Table 4 shows the oxide composition of the fly ash used. This material mostly contains SiO_2 and Al_2O_3 . The analysis of the oxide composition showed that this material also contains oxides of iron, potassium, calcium, manganese, and titanium. Titanium in geopolymeric materials affects plasticity but is most often considered an impurity. Other scientific studies revealed the nucleating activity of the crystallization process in the geopolymerization process [36–39].

Table 4. Oxide composition of fly ash.

Oxide Composition	SiO_2	Al_2O_3	Fe_2O_3	K_2O	CaO	MgO	TiO_2	Na_2O	P_2O_5	SO_2
Fly ash	49.69%	24.84%	7.20%	3.59%	3.77%	1.52%	1.13%	1.88%	0.33%	0.96%

Base materials were also tested using a particle size analyzer, and the results are presented in Table 5 and Figure 1. The mean size of fly ash was equal to around $17 \mu\text{m}$, while river sand was found to be larger, and its mean particle size was approximately $730 \mu\text{m}$.

Table 5. The particle size of based materials.

D-Values	Fly Ash	River Sand
D_{10} (μm)	2.208	400.776
D_{50} (μm)	12.268	647.689
D_{90} (μm)	36.175	1036.757
Mean size (μm)	16.975	730.226

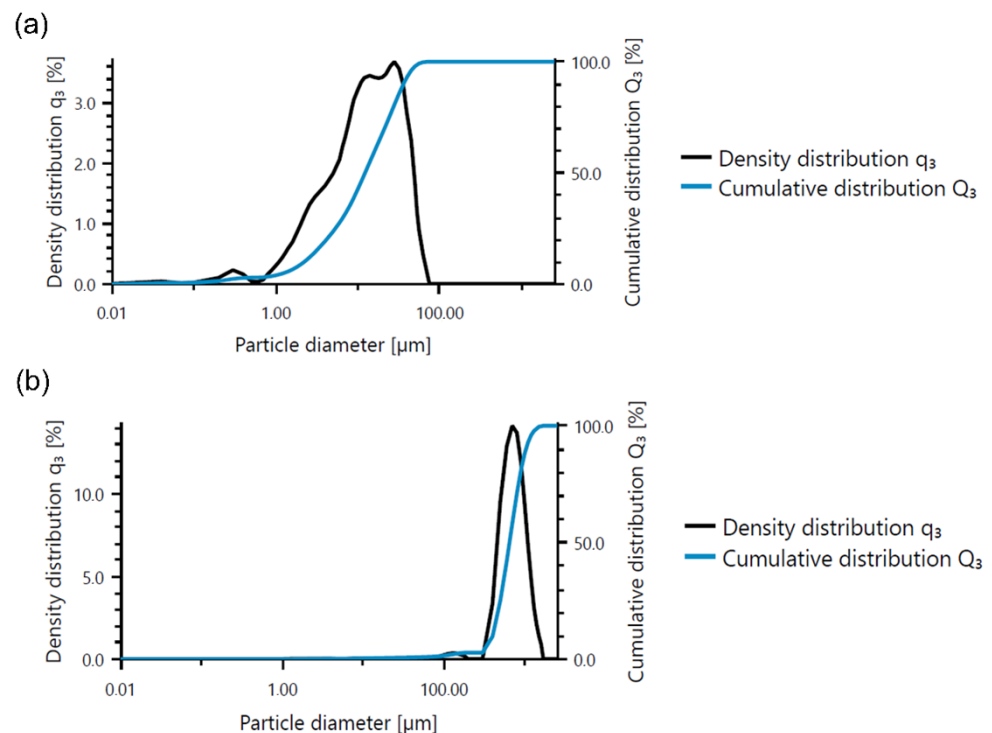


Figure 1. Analysis of particle size of based materials: (a) fly ash and (b) river sand.

The first stage of the research was the selection of the spray gun nozzle. As part of the selection process of the appropriate nozzle, a nozzle with a diameter of $4 \times 10^{-3} \text{ m}$ to

8×10^{-3} m was tested, using the medium working range of the gun pressure (0.51–0.65 MPa). The material was spread from a distance of 0.25 m. The first results when using a nozzle with a diameter of 8×10^{-3} m provided satisfactory results. However, the sprayed layer was too thick, and the sprayed material ran off the pad, resulting in an uneven and irregular surface (Figure 2c). The use of a nozzle with a diameter of 6×10^{-3} m contributed to better results than a nozzle with a larger diameter. The spraying process was correct. A reduction in the nozzle diameter limited the material spread, resulting in a more uniform and even layer of the geopolymer material. The final effect had much better quality than the material sprayed with the 8×10^{-3} m nozzle (Figure 2b). The last sample of the tested nozzle diameters was the one with a diameter of 4×10^{-3} m. The spray test showed that this diameter was too small for the consistency of the geopolymeric mass, creating a back pressure that resulted in the supply system being blocked, thus restricting the flow (Figure 2a). Based on the conducted research, the nozzles with a diameter of 6×10^{-3} m were selected for further investigation.

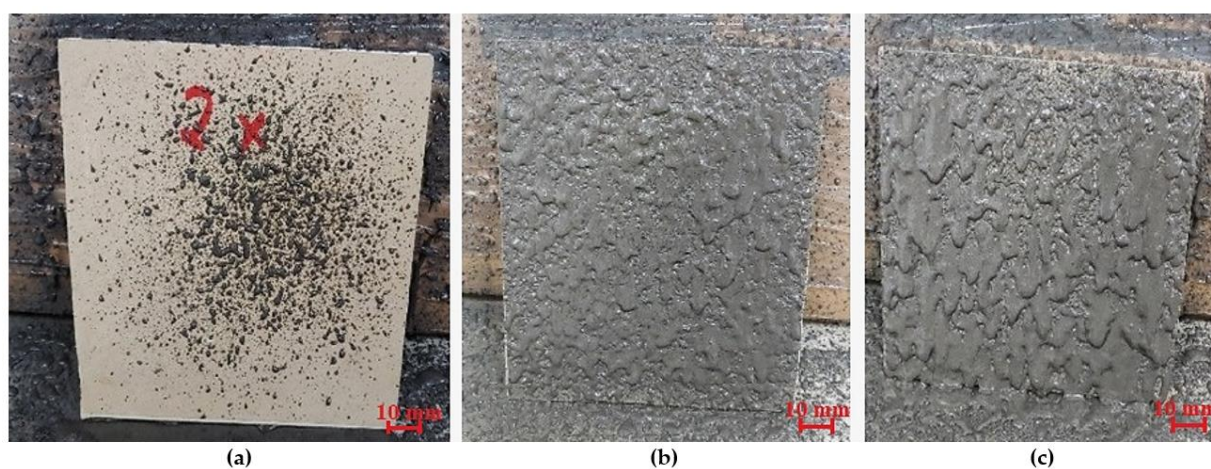


Figure 2. Geopolymer layer using a spray nozzle: (a) with a diameter of 4×10^{-3} m, (b) with a diameter of 6×10^{-3} m, and (c) with a diameter of 8×10^{-3} mm.

After selecting the optimal diameter of the spray nozzle, we proceeded to obtain the optimal working pressure of the spray. Table 6 shows the results of spraying the geopolymer layers. As shown in Table 3, and with the help of a pressure gauge, the pressure ranges at which it was possible to operate the spray gun were determined. With the low-pressure range of the spray gun, it was impossible to apply the geopolymer (similar to the situation with the smallest diameter nozzle). For other geopolymer mixtures, spray gun operation was possible. The obtained visual results of the geopolymer layers applied by using the spraying method are shown in Table 6.

The foaming process and the macrostructure of geopolymer foams depend on the foaming agent used. During the foaming process, the blowing agent, mixing conditions, the number of additives, and the temperature determine the foamed material obtained. The process of foaming with hydrogen peroxide and aluminum powder is mainly based on the release of hydrogen. This gas is responsible for forming a porous structure [40–42].

The first material applied was a geopolymer material foamed with hydrogen peroxide (Mix 1). The foaming agent was introduced at the end of mixing the geopolymer mixture to ensure the longest time for the spraying process. This solution was chosen because the reaction of hydrogen peroxide was immediate and, despite the maximally delayed addition of H_2O_2 , it had already occurred in the mixer. Geopolymer foam spreading was carried out at two different operating pressure ranges of the spray gun (Table 3). First, the maximum pressure operating range was used. Analysis of the results showed that the sprayed layers were characterized by a smooth surface and little visible foaming effect. This effect is related to the foaming reaction that had already occurred in the mixer, and the relatively high spray pressure destroyed the foamed structure.

Table 6. Working pressure range of the 6×10^{-3} m spray nozzle for geopolymer materials.

	Mix 1	Mix 2
Low pressure	No spraying of the geopolymer coating is possible.	No spraying of the geopolymer coating is possible.
Medium pressure		
High pressure		

An attempt was then made to apply the geopolymer coating, this time in the medium pressure range. The foaming effect of the sprayed geopolymer layer was more evident on the surface than when working at high pressure. It can be seen that the geopolymer material flowed down the vertical wall, forming the so-called streaks. The foaming effect was more pronounced in this case than that obtained under high working pressure.

The addition of aluminum powder (Mix 2) was used as an alternative method of foaming the geopolymer. The foaming agent was introduced as the last component of the geopolymer mix before the spraying process itself. Aluminum powder is a foaming agent that reacts more slowly than hydrogen peroxide. The addition of aluminum slightly changed the consistency, making the geopolymer slightly denser. Using the high working pressure range of the spray gun, once the geopolymer foam was applied to the surfaces, the foamed structure was destroyed (Table 6). Furthermore, the applied layer was characterized by a lumpy, heterogeneous texture. The application process of Mix 2, using the medium pressure range of the spray gun, produced a less satisfactory result than the other application attempts. Although foaming only occurred on half of the surfaces, it can be concluded that the process occurred after the material was applied with the air gun. In addition, the applied surface that was foamed showed good bonding properties to the base surface, i.e., it did not run off the vertical wall. The obtained results led the authors to consider other possible options for applying geopolymer coatings using an air gun. The research carried out at this stage aimed to determine the feasibility of using readily available methods to produce the foamed layers, which would facilitate applications in the construction industry. Knowing that aluminum causes delayed foaming [43], tests were carried out using an aluminum layer as a primer (Figure 3).

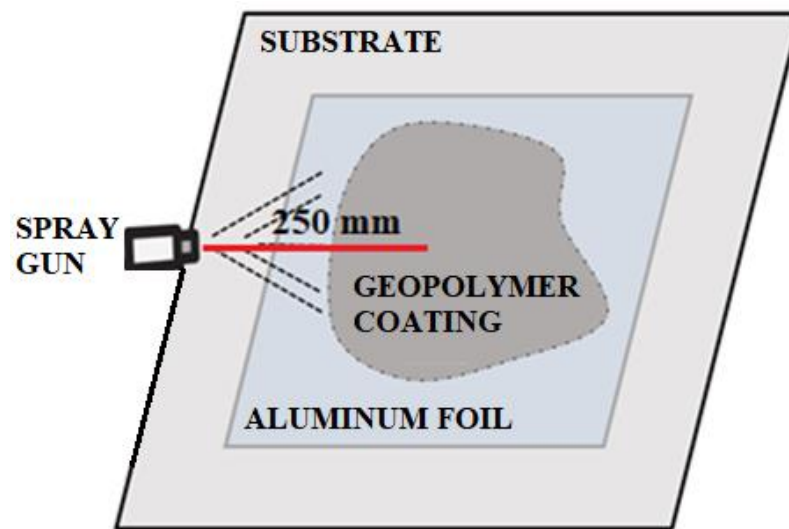


Figure 3. Scheme of applied material on aluminum foil.

A geopolymer base without foaming agents was then sprayed onto the film. The layer was still relatively thin, but it was possible to achieve a foaming effect after spraying, as shown in Figure 4.

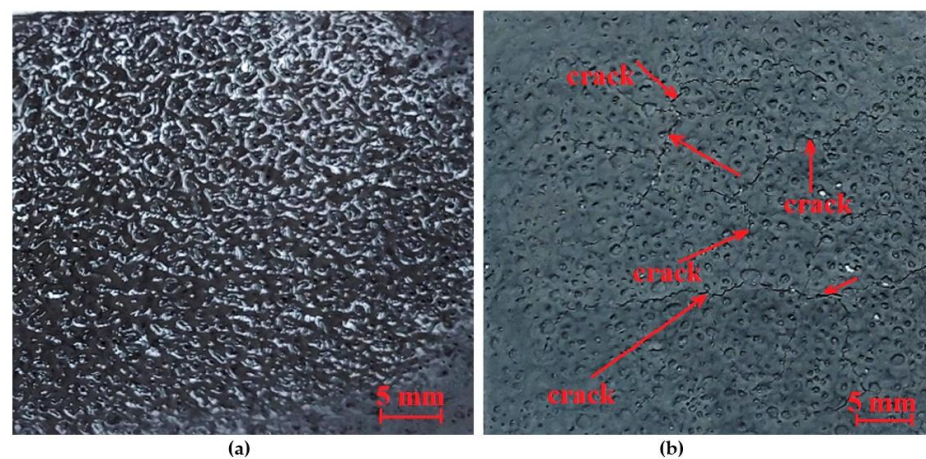


Figure 4. Foamed geopolymer layer sprayed on an aluminum foil: (a) foaming effect after partial drying, (b) foaming effect after complete drying with visible cracks.

The produced layer did not meet expectations, as cracks appeared after the layer dried. Therefore, as part of this research, it was decided to use the manual method of applying the layer. The manual technique allows for the application of a denser geopolymer, which reduces the number of cycles required. The proportions of the ingredients were the same as before (Mix 2). The addition of aluminum powder was 1 g, which did not cause excessive brittleness and was evenly distributed during the mixing process. This was the only test that was entirely successful, giving a foam layer that was still completely free of cracks and brittleness after 24 h. The resulting layer was subjected to thermal conductivity tests. The test results are presented in Table 7. Due to the application of the layer on a cardboard substrate, a thermal conductivity test was conducted on both the cardboard and the layer applied to the cardboard.

Thermal conductivity tests showed that the foamed material applied to the pad had a thermal conductivity of 0.155 (W/(m × K)).

Table 7. Thermal conductivity and thermal resistance of the manufactured sample.

Material	Mean Temp. (K)	Delta Temp. (K)	Thermal Conductivity (W/(m·K))	Load Pressure (kPa)
Cardboard	283.15	20.0	0.04169	2.0
Geopolymer layer (Mix 2) on the cardboard	283.15	20.0	0.15545	0.6

Porosity plays a critical role in the conductivity of materials. The greater the number of pores in materials, the higher the amount of enclosed air in the structure. This relation causes lower thermal conductivity. Research on geopolymeric materials foamed with aluminum powder or hydrogen peroxide showed that the conductivity of this type of material ranges from 0.07 to 0.22 (W/(m × K)) [44–47]. The obtained results were within this given range, but it should be emphasized that the produced layer was very thin, and the test results indicate the potential of this type of application.

The results presented here show that the air spraying method of geopolymers using a cup gun is potentially applicable. However, the focus should be on the selection of a suitable mixture of foamed geopolymer and additives to stabilize the foaming process after the layer is applied to the substrate. In this paper, basic blends of foamed geopolymers were presented, without any hydraulic additives or stabilizers that could affect the foaming and setting of the geopolymer. The problem of the application of foamed geopolymers is very important, as the development of an application method for such material would allow the industrial use of geopolymers as insulation materials. Currently, it is only possible to produce these materials in molds.

The authors decided to carry out tests on foamed geopolymers obtained by using the mold casting method, the material composition of which was the same as that of the geopolymers applied by spraying (Mix 1 and Mix 2). The performance of the foaming process obtained by casting the foamed geopolymer masses into molds was significantly better than that of the spraying method. The thermal conductivity values of the foamed geopolymers (Mix 1 and Mix 2) cured in the mold are shown in Table 8.

Table 8. Thermal conductivity of the manufactured sample.

Material	Mean Temp. (K)	Delta Temp. (K)	Thermal Conductivity [W/(m·K)]	Load Pressure (kPa)
Mix 1	283.15	20.0	0.12493	2.2
Mix 2	283.15	20.0	0.12581	2.2

The thermal conductivity coefficient for the foamed geopolymer, Mix 1, was 0.12493 (W/(m·K)). In contrast, the foamed geopolymer Mix 2 achieved a slightly higher thermal conductivity value of 0.12581 (W/(m·K)). For the geopolymer foams based on fly ash and metakaolin, Wu et al. obtained thermal conductivity coefficient results oscillating in the range of 0.06–0.09 (W/(m × K)) [48]. In turn, in their work, Łach et al. obtained the thermal conductivity results of 0.08 (W/(m × K)) for foamed geopolymers based on fly ash and marshmallow, modified with gypsum and the stabilizing agent Mn 575 [44]. Zhang et al. focused in their work on testing different variants of fly ash-based foamed geopolymers. After performing thermal conductivity tests for the above materials, they obtained results in the range of 0.15 (W/(m × K)) to 0.48 (W/(m × K)) [49]. It is important to strive for such parameters with spraying application, so any trials and achievements in this area are very important.

Figure 5 shows the average compressive strength results for the foamed geopolymers obtained (Mix 1 and Mix 2) by using mold casting technology.

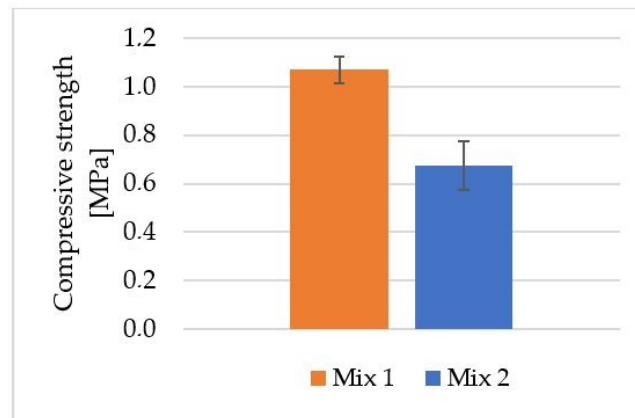


Figure 5. Average compressive strength for geopolymer material obtained via mold casting method.

A geopolymer based on fly ash and river sand foamed with H_2O_2 (Mix 1) achieved an average compressive strength of 1.1 MPa. The average compressive strength for the geopolymer foamed with aluminum powder (Mix 2) was approximately 0.7 MPa. This is a decrease in compressive strength of approximately 36% compared with the geopolymer foamed with H_2O_2 . In their study, Kurtuluş et al. investigated the compressive strength of geopolymer foams based on fly ash and metakaolin, cured at different temperatures. H_2O_2 was used as a foaming additive in this case. The materials obtained in their work had compressive strengths ranging from 1.14 to 1.78 MPa [50]. Krzywoń and Dawczyński investigated the strength parameters of foamed geopolymer reinforced with GFRP mesh in their study. The results obtained for foamed geopolymers reinforced with GFRP mesh oscillated between 0.68 MPa and 9.14 MPa [51]. Huang et al. obtained compressive strength results for ultra-lightweight Portland cement-based foam concrete of 0.8–1.1 MPa [52].

Scanning electron microscopy (SEM) allows for the visual examination of a material to obtain information about its surface topography. In addition, it allows for the identification of the structures formed that cannot be revealed by other examination methods [53,54].

Figure 6 shows the microstructure of the foamed geopolymers based on fly ash and sand after the compressive strength test.

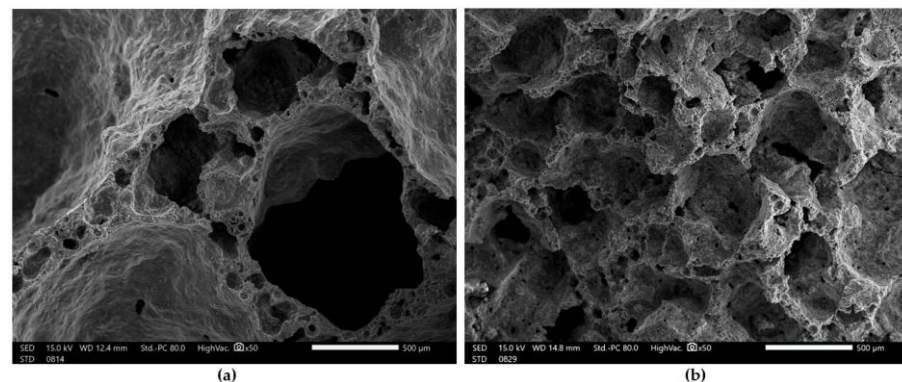


Figure 6. SEM images of foamed geopolymer materials at 50× magnification: (a) Mix 1; (b) Mix 2.

Figure 6a shows the microstructure of fly ash and the sand-based geopolymer material foamed with H_2O_2 . In addition to the macropores, which ranged in size from 2 to 3 mm, smaller pores could also be observed, which ranged in size from 10 to 300 μm . Figure 6b shows the microstructure of the geopolymer material based on fly ash and sand, foamed with aluminum powder. Compared with the material foamed with H_2O_2 , this geopolymer foam had a more uniform pore size in its structure, which oscillated around 500 μm . We obtained a very similar microstructure to the geopolymers studied by another group of scientists [55,56].

4. Conclusions

The main objective of this study was to test the feasibility of using additive spray technology to apply foamed geopolymer coatings to structures and vertical surfaces. The spray application technology eliminates the challenges of protecting surfaces with irregular geometries and, in addition, can increase the applications of geopolymers as an insulating material. Tests were conducted to investigate the possibility of using an air gun with variable nozzles to apply layers of foamed geopolymers. A visual assessment, which consisted of evaluating the adhesion of the applied material to the substrate and the degree of foaming in the applied geopolymer layer on the vertical surface, indicated that the best solution was to use a medium working pressure of the spray nozzle (0.51–0.65 MPa) and to choose a nozzle diameter of 6×10^{-3} m. The low-pressure range of the spray nozzle, irrespective of the nozzle diameter, was unsuitable for the application of foamed geopolymer mixtures to the vertical surfaces (0.4–0.5 MPa). The use of high spray nozzle operating pressures was also unsuitable (0.66–0.8 MPa). In this study, basic mixtures for foamed geopolymers were used, which, during the spraying process itself, slightly lost their foaming properties; thus, foaming was less effective than when the foamed geopolymers were obtained via mold casting. The geopolymer foamed with H₂O₂ at medium spray nozzle operating pressure had the best foaming effect when sprayed onto the vertical surface. The problem, however, was that the geopolymer mass took too long to set in the air, and gravitational force caused some streaking of the freshly applied material. However, the effect is very promising, and the modification of mixes with hydraulic additives or stabilizers can have a positive influence on the foaming process and the setting time of the geopolymer in air. The aluminum powder used to foam the material also showed its potential use in the spray application of foamed geopolymers. The foaming effect was slightly less than for foamed geopolymer with H₂O₂, but the resulting surface was more regular, and there was no pooling of the material along the vertical wall.

Author Contributions: Conceptualization, M.L. and K.K.; methodology, M.L. and K.K.; validation, M.L. and K.K.; formal analysis, K.K.; investigation, K.K. and K.P.; resources, M.L.; writing—original draft preparation, K.K. and K.P.; writing—review and editing, M.L., B.K. and P.B.; visualization, K.K. and P.B.; supervision, M.L. and B.K.; project administration, M.L.; funding acquisition, M.L. All authors have read and agreed to the published version of the manuscript.

Funding: This research was funded by the National Center for Research and Development under the Grant: Development of technology for additive production of environmentally friendly and safe insulation materials and ability to accumulate heat based on the alkaline activation of anthropogenic raw materials (LIDER/16/0061/L-11/19/NCBR/2020).

Institutional Review Board Statement: Not applicable.

Informed Consent Statement: Not applicable.

Data Availability Statement: Not applicable.

Conflicts of Interest: The authors declare no conflict of interest.

References

1. Amran, Y.M.; Alyousef, R.; Alabduljabbar, H.; El-Zeadani, M. Clean production and properties of geopolymer concrete: A review. *J. Clean. Prod.* **2020**, *251*, 119679. [[CrossRef](#)]
2. Cong, P.; Cheng, Y. Advances in geopolymer materials: A comprehensive review. *J. Traffic Transp. Eng.* **2021**, *8*, 283–314. [[CrossRef](#)]
3. Ma, C.K.; Awang, A.Z.; Omar, W. Structural and material performance of geopolymer concrete: A review. *Constr. Build. Mater.* **2018**, *186*, 90–102. [[CrossRef](#)]
4. Gao, B.; Jang, S.; Son, H.; Lee, H.J.; Lee, H.J.; Yang, J.J.; Bae, C.J. Study on mechanical properties of kaolin-based geopolymer with various Si/Al ratio and aging time. *J. Korean Ceram. Soc.* **2020**, *57*, 709–715. [[CrossRef](#)]
5. Ayeni, O.; Onwualu, A.P.; Boakye, E. Characterization and mechanical performance of metakaolin-based geopolymer for sustainable building applications. *Constr. Build. Mater.* **2021**, *272*, 121938. [[CrossRef](#)]
6. Kaur, K.; Singh, J.; Kaur, M. Compressive strength of rice husk ash based geopolymer: The effect of alkaline activator. *Constr. Build. Mater.* **2018**, *169*, 188–192. [[CrossRef](#)]
7. Firdous, R.; Stephan, D.; Djobo, J.N.Y. Natural pozzolan based geopolymers: A review on mechanical, microstructural and durability characteristics. *Constr. Build. Mater.* **2018**, *190*, 1251–1263. [[CrossRef](#)]

8. Fan, F.; Liu, Z.; Xu, G.; Peng, H.; Cai, C.S. Mechanical and thermal properties of fly ash based geopolymers. *Constr. Build. Mater.* **2018**, *160*, 66–81. [[CrossRef](#)]
9. Zhang, Y.; Xiao, R.; Jiang, X.; Li, W.; Zhu, X.; Huang, B. Effect of particle size and curing temperature on mechanical and microstructural properties of waste glass-slag-based and waste glass-fly ash-based geopolymers. *J. Clean. Prod.* **2020**, *273*, 122970. [[CrossRef](#)]
10. Aziz, A.; Stocker, O.; El Hassani, I.E.E.A.; Laborier, A.P.; Jacotot, E.; El Khadiri, A.; El Bouari, A. Effect of blast-furnace slag on physicochemical properties of pozzolan-based geopolymers. *Mater. Chem. Phys.* **2021**, *258*, 123880. [[CrossRef](#)]
11. Aziz, I.H.; Abdullah, M.M.A.B.; Salleh, M.M.; Azimi, E.A.; Chaiprapa, J.; Sandu, A.V. Strength development of solely ground granulated blast furnace slag geopolymers. *Constr. Build. Mater.* **2020**, *250*, 118720. [[CrossRef](#)]
12. Jindal, B.B.; Sharma, R. The effect of nanomaterials on properties of geopolymers derived from industrial by-products: A state-of-the-art review. *Constr. Build. Mater.* **2020**, *252*, 119028. [[CrossRef](#)]
13. Sindhunata; Van Deventer, J.S.J.; Lukey, G.C.; Xu, H. Effect of curing temperature and silicate concentration on fly-ash-based geopolymerization. *Ind. Eng. Chem. Res.* **2006**, *45*, 3559–3568. [[CrossRef](#)]
14. Shin, S.; Goh, G.; Lee, C. Predictions of compressive strength of GPC blended with GGBFS developed at varying temperatures. *Constr. Build. Mater.* **2019**, *206*, 1–9. [[CrossRef](#)]
15. Yaseri, S.; Hajiaghahi, G.; Mohammadi, F.; Mahdikhani, M.; Farokhzad, R. The role of synthesis parameters on the workability, setting and strength properties of binary binder-based geopolymer paste. *Constr. Build. Mater.* **2017**, *157*, 534–545. [[CrossRef](#)]
16. Lahoti, M.; Wong, K.K.; Yang, E.H.; Tan, K.H. Effects of Si/Al molar ratio on strength endurance and volume stability of metakaolin geopolymers subject to elevated temperature. *Ceram. Int.* **2018**, *44*, 5726–5734. [[CrossRef](#)]
17. Nath, P.; Sarker, P.K. Flexural strength and elastic modulus of ambient-cured blended low-calcium fly ash geopolymer concrete. *Constr. Build. Mater.* **2017**, *130*, 22–31. [[CrossRef](#)]
18. Kope, R.A.; Pralat, K.; Ciemnicka, J.; Buczkowska, K. Influence of the calcination temperature of synthetic gypsum on the particle size distribution and setting time of modified building materials. *Energies* **2020**, *13*, 5759. [[CrossRef](#)]
19. Figiela, B.; Šimonová, H.; Korniejenco, K. State of the art, challenges, and emerging trends: Geopolymer composite reinforced by dispersed steel fibers. *Rev. Adv. Mater. Sci.* **2022**, *61*, 1–15. [[CrossRef](#)]
20. Korniejenco, K.; Figiela, B.; Ziejewska, C.; Marczyk, J.; Bazan, P.; Hebda, M.; Choińska, M.; Lin, W.-T. Fracture behavior of long fiber reinforced geopolymer composites at different operating temperatures. *Materials* **2022**, *15*, 482. [[CrossRef](#)]
21. Görhan, G.; Kürklü, G. The influence of the NaOH solution on the properties of the fly ash-based geopolymer mortar cured at different temperatures. *Compos. Part B Eng.* **2014**, *58*, 371–377. [[CrossRef](#)]
22. Nguyen, L.; Moseson, A.J.; Farnam, Y.; Spataro, S. Effects of composition and transportation logistics on environmental, energy and cost metrics for the production of alternative cementitious binders. *J. Clean. Prod.* **2018**, *185*, 628–645. [[CrossRef](#)]
23. Temuujin, J.; Minjigmaa, A.; Rickard, W.; Lee, M.; Williams, I.; Van Riessen, A. Fly Ash Based Geopolymer Thin Coatings on Metal Substrates and Its Thermal Evaluation. *J. Hazard. Mater.* **2010**, *180*, 748–752. [[CrossRef](#)] [[PubMed](#)]
24. Yong, S.L.; Feng, D.W.; Lukey, G.C.; Van Deventer, J.S.J. Chemical Characterisation of The Steel Geopolymeric Gel Interface. *Colloids Surf. A Physicochem. Eng. Asp.* **2007**, *302*, 411–423. [[CrossRef](#)]
25. Balaguru, P.N.; Nazier, M.; Arafa, M. *Field Implementation of Geopolymer Coatings*; New Jersey Department of Transportation: Ewing Township, NJ, USA, 2008. Available online: <https://cait.rutgers.edu/wp-content/uploads/2018/05/fhwa-nj-2002-011.pdf> (accessed on 12 August 2022).
26. Zhang, Z.; Yao, X.; Zhu, H. Potential Application of Geopolymers as Protection Coatings for Marine Concrete I. Basic Properties. *Appl. Clay Sci.* **2010**, *49*, 67–68.
27. Zhang, Z.; Yao, X.; Zhu, H. Potential application of geopolymers as protection coatings for marine concrete: II Microstructure and anticorrosion mechanism. *Appl. Clay Sci.* **2010**, *49*, 7–12. [[CrossRef](#)]
28. Tian, Q.; Wang, S.; Sui, Y.; Lv, Z. Alkali-activated materials as coatings deposited on various substrates: A review. *Int. J. Adhes. Adhes.* **2021**, *110*, 102934. [[CrossRef](#)]
29. Temuujin, J.; Minjigmaa, A.; Rickard, W.; Lee, M.; Williams, I.; Van Riessen, A. Preparation of metakaolin based geopolymer coatings on metal substrates as thermal barriers. *Appl. Clay Sci.* **2009**, *46*, 265–270. [[CrossRef](#)]
30. McAlorum, J.; Perry, M.; Vlachakis, C.; Biondi, L.; Lavoie, B. Robotic spray coating of self-sensing metakaolin geopolymer for concrete monitoring. *Autom. Constr.* **2021**, *121*, 103415. [[CrossRef](#)]
31. Lu, B.; Zhu, W.; Weng, Y.; Liu, Z.; Yang, E.H.; Leong, K.F.; Qian, S. Study of MgO-activated slag as a cementless material for sustainable spray-based 3D printing. *J. Clean. Prod.* **2020**, *258*, 120671. [[CrossRef](#)]
32. Zhang, Z.; Yao, X.; Wang, H. Potential application of geopolymers as protection coatings for marine concrete III: Field experiment. *Appl. Clay Sci.* **2012**, *67–68*, 57–60. [[CrossRef](#)]
33. Deshmukh, K.; Parsai, R.; Anshul, A.; Singh, A.; Bhardwaj, P.; Gupta, R.; Mishra, D.; Amritphale, S.S. Studies on fly ash based geopolymeric material for coating on mild steel by paint brush technique. *Int. J. Adhes. Adhes.* **2017**, *75*, 139–144. [[CrossRef](#)]
34. Bhardwaj, P.; Gupta, R.; Deshmukh, K.; Mishra, D. Optimization studies and characterization of advanced geopolymer coatings for the fabrication of mild steel substrate by spin coating technique. *Indian J. Chem. Technol.* **2021**, *28*, 59–76. Available online: <https://op.niscair.res.in/index.php/IJCT/article/view/31721> (accessed on 12 August 2022).
35. Provis, J.L.; Van Deventer, J.S. *Geopolymers—Structure, Processing, Properties, and Industrial Application*; Woodhead Publishing in Materials: Oxford, UK, 2009; pp. 310–311.

36. Lizcano, M.; Gonzalez, A.; Basu, S.; Lozano, K.; Radovic, M. Effects of water content and chemical composition on structural properties of alkaline activated metakaolin-based geopolymers. *J. Am. Ceram. Soc.* **2012**, *95*, 2169–2177. [[CrossRef](#)]
37. Perera, D.S.; Vance, E.; Finnie, K.S.; Blackford, M.G.; Cassidy, D.J. Disposition of water in Metakaolinite based geopolymers. *Adv. Ceram. Matrix Compos.* **2006**, *75*, 225–236.
38. Song, Z.L.; Ma, L.Q.; Wu, Z.J.; He, D.P. Effects of viscosity on the cellular structure of foamed aluminum in the foaming process. *J. Mater. Sci.* **2000**, *35*, 15–20. [[CrossRef](#)]
39. Chindaprasirt, P.; Chareerat, T.; Sirivivatnanon, V. Workability, and strength of coarse high calcium fly ash geopolymer. *Cem. Concr. Compos.* **2007**, *29*, 224–229. [[CrossRef](#)]
40. Ercoli, R.; Laskowska, D.; Nguyen, V.V.; Le, V.S.; Louda, P.; Łoś, P.; Ciemnicka, J.; Prałat, K.; Renzulli, A.; Paris, E.; et al. Mechanical and thermal properties of geopolymer foams (GFs) doped with by-products of the secondary aluminum industry. *Polymers* **2022**, *14*, 703. [[CrossRef](#)]
41. Nguyen, V.V.; Le, V.S.; Louda, P.; Szczypiński, M.M.; Ercoli, R.; Vojtěch, R.; Łoś, P.; Prałat, K.; Plaskota, P.; Pacyniak, T.; et al. Low-density geopolymer composites for the construction industry. *Polymers* **2022**, *14*, 304. [[CrossRef](#)]
42. Novais, R.M.; Ascensão, G.; Buruberry, L.H.; Senff, L.; Labrincha, J.A. Influence of blowing agent on the fresh- and hardened-state properties of lightweight geopolymers. *Mater. Des.* **2016**, *108*, 551–559. [[CrossRef](#)]
43. Łach, M. Geopolymer Foams—Will They Ever Become a Viable Alternative to Popular Insulation Materials?—A Critical Opinion. *Materials* **2021**, *14*, 3568. [[CrossRef](#)] [[PubMed](#)]
44. Łach, M.; Pławicka, K.; Bąk, A.; Lichočka, K.; Korniejenko, K.; Cheng, A.; Lin, W.-T. Determination of the influence of hydraulic additives on the foaming process and stability of the produced geopolymer foams. *Materials* **2021**, *14*, 5090. [[CrossRef](#)] [[PubMed](#)]
45. Wongsā, A.; Sata, V.; Nuaklong, P.; Chindaprasirt, P. Use of crushed clay brick and pumice aggregates in lightweight geopolymer concrete. *Constr. Build. Mater.* **2018**, *188*, 1025–1034. [[CrossRef](#)]
46. Demirboğa, R.; Gül, R. The effects of expanded perlite aggregate, silica fume and fly ash on the thermal conductivity of lightweight concrete. *Cem. Concr. Res.* **2003**, *33*, 723–727. [[CrossRef](#)]
47. Cui, C.; Wang, D. Effects of Water on Pore Structure and Thermal Conductivity of Fly Ash-Based Foam Geopolymers. *Adv. Mater. Sci. Eng.* **2019**, *2019*, 3202794. [[CrossRef](#)]
48. Wu, J.; Zhang, Z.; Zhang, Y.; Li, D. Preparation and characterization of ultra-lightweight foamed geopolymer (UFG) based on fly ash-metakaolin blends. *Constr. Build. Mater.* **2018**, *168*, 771–779. [[CrossRef](#)]
49. Zhang, Z.; Provis, L.J.; Reid, A.; Wang, H. Mechanical, thermal insulation, thermal resistance and acoustic absorption properties of geopolymer foam concrete. *Cem. Concr. Compos.* **2015**, *62*, 97–105. [[CrossRef](#)]
50. Kurtuluş, C.; Baspınar, M.S. Development of Efflorescence Control Methods of Fly Ash Based Foam Geopolymers. *AKU J. Sci. Eng.* **2020**, *20*, 129–137. [[CrossRef](#)]
51. Krzywoń, R.; Dawczyński, S. Strength Parameters of Foamed Geopolymer Reinforced with GFRP Mesh. *Materials* **2021**, *14*, 689. [[CrossRef](#)]
52. Huang, Z.; Zhang, T.; Wen, Z. Proportioning and characterization of Portland cement-based ultra-lightweight foam concretes. *Constr. Build. Mater.* **2015**, *79*, 390–396. [[CrossRef](#)]
53. Pławicka, K.; Bazan, P.; Lin, W.-T.; Korniejenko, K.; Sitarz, M.; Nykiel, M. Development of Geopolymers Based on Fly Ashes from Different Combustion Processes. *Polymers* **2022**, *14*, 1954. [[CrossRef](#)] [[PubMed](#)]
54. Kang, X.; Gan, Y.; Chen, R.; Zhang, C. Sustainable eco-friendly bricks from slate tailings through geopolymerization: Synthesis and characterization analysis. *Constr. Build. Mater.* **2021**, *278*, 122337. [[CrossRef](#)]
55. Su, Z.; Hou, W.; Sun, Z.; Lv, W. Study of In Situ Foamed Fly Ash Geopolymer. *Materials* **2020**, *13*, 4059. [[CrossRef](#)] [[PubMed](#)]
56. Kristály, F.; Szabó, R.; Mádai, F.; Debreczeni, Á.; Mucsi, G. Lightweight composite from fly ash geopolymer and glass foam. *J. Sustain. Cem. Based Mater.* **2021**, *10*, 1–22. [[CrossRef](#)]